PAPER

Check for updates

Nano-particle transport and the prediction of a valid area to be trapped based on a plasmonic antenna array

Chang-gui Lu, [ID]†* Xue-fang Hu,† Ze-rong Yuan and Yi-ping Cui [ID]

Optical antennas are promising for optical trapping and particle manipulation, when converting light between localized energy and freely propagating radiation. In this paper, we proposed a numerical method for the transport of nanoparticles using the optical force field over a plasmonic Au antenna array. The plasmonic Au antenna array is designed to produce strong near-field hot spots when illuminated by a plane wave. The hot spots function as optical traps, separately addressable by their resonant wavelengths. By changing the traps sequentially, the nanoparticles can be handed off between adjacent traps. We also demonstrated a valid area in which the nanoparticles could be trapped and transferred stably by discussing the trapping potential that particles encountered. The simulated and calculated results showed that this method had promising applications in the field of biochemical diagnoses and high-accuracy optical manipulation.

1. Introduction

Optical tweezers have found tremendous application in various areas, including colloidal sciences, chemistry, and biophysics since their invention several decades ago.[1–5] However, high numerical aperture and large incident intensity are required to get enough optical force when nanoparticles need to be manipulated. This also may damage the biological cell or specimen due to the heat generated by large incident power.[6,7] As the metal surface plasmon resonance structures with localized strong gradient electric fields can be used to optically trap nanoparticles,[8–13] many groups have focused on the optical trapping for a long time.[14–16] The optical force on the nanoparticles caused by the evanescent field can draw the nanoparticles into a 'hot spot'. The structures that are used to produce the 'hot spots' are various, such as coaxial plasmonic apertures,[17] optical antennas[18] and hybrid plasmonic waveguides.[19]

In recent years, several studies have demonstrated the promise of plasmonic optical trapping and transport.[20–22] For example, Kai Wang and his colleagues had proposed a method to trap and rotate the nanoparticles. In his letter, although the gold pillars can be used to trap and rotate the nanoparticles, but the nanoparticles just rotate around the gold pillars, not a long distance transport.[10] Paul Hansen proposed a C-shape nanostructures with different sizes to realize nanoparticles transport. Nanoparticles may be handed off between adjacent traps which

separately addressable by the resonant wavelengths and polarizations.[23,24] Zhiwen Kang proposed a similar plasmonic system consisting of graded sizes nanodisks. Nanoparticles can be transferred from one disk to another disk by switching excitation wavelength.[25] However, Shuang Zhang and his colleagues have proposed a plasmonic array structure with varying lengths Au antennas in his paper. It showed that the gold thin-film antennas could be used to control light at the nanoscale.[26] As the resonant wavelength is related to the length of the antenna closely, it enable the Au antenna a potential application in the optical trapping, biochemical diagnose and high-accuracy optical manipulation. Although trap and transport the particles can be realized effortless, what attract our attention is the valid area in which the particles can be trapped. Thus, a further study about the application of this Au antennas and make a prediction about the valid area in which the particles can be trapped is of great significance.

In this paper, we numerically designed a plasmonic Au antenna array as a conveyor belt to transport the particle by changing the resonant wavelength, the transporting distance is about 270 nm, and we also predicted the valid area in which the particles can be trapped stably. Although many research have been focused to trap and transport the particles, but it is rare to predict the valid area in which the particles can be trapped, if we can predict the valid area where the particles can be trapped, it can be used to avoid the waste of the cell or protein in the experiment and improved the efficiency greatly, which makes this work very meaningful. This method may provide a path toward the biochemical diagnose or high-accuracy optical manipulation.

Advanced Photonics Center, School of Electronic Science & Engineering, Southeast University, Nanjing, Jiangsu, 210096, China. E-mail: changguilu@seu.edu.cn

† These authors contributed equally to this work.

2. Model

The schematic of the plasmonic Au antenna array is shown in Fig. 1(a), it consists of four optical dipole antennas which have a slight difference in length. Each antenna can focus the incident light into the small gap in the middle of the antenna couple. The gap area is seen as a 'hot spot' which can be used to trap nanoparticles. However, it is different from the common method when several antennas are combined to make up a system. As is shown in Fig. 1(b), the lengths of the antennas are 170 nm, 200 nm, 230 nm, 260 nm respectively. The resonant wavelength is related to the length of the antenna closely, and the gradually changed antennas are similar to a trapezoid. The width and thickness of the all antennas are 50 nm and 30 nm. The gap between nearest antennas is 35 nm and the distance between two arms is 40 nm. The value of gap between nearest antennas is of great important because an ideal value can ensure a larger capture range and a lower interference between antennas. On account of the technological reason, it is unlikely to make the edges of antennas sharp perfectly. Thus, the edges of the antenna are set as the fillets to reflect the reality closely. The curvature radius of the rounding antenna edges is 15 nm. The finite-element method is employed to calculate the optical response of the plasmonic system under the illumination of a normal incident plane wave with the electric field X-polarized. The perfect matching layers are set to the absorption boundary.

The nanostructure consists of four Au antennas on the glass substrate, they are distributed independent but coupled with each other. The surrounding liquid environment is the water (n

$= 1.33$). The relative permittivity of Au is from ED Palik's data.[27] Mutual coupling exists in the adjacent antennas and it is the reason why we choose such a complex structure. When the optical responses of antennas are analyzed independently, as shown in Fig. 1(c), there is no coupling effect between adjacent antennas, but the interference is obvious. Take the antenna 1 for example, the field enhancement of antenna 2 is also tremendous at the resonant wavelength of antenna 1, which hindered the transport of the particle at the point A. However, when mutual coupling effect is taken into account, things are different. As is shown in Fig. 1(d), take the antenna 1 for example as before, the field enhancement of antenna 2 can be ignored at the resonant wavelength of antenna 1, the resonant antenna suppresses the other non-resonant antennas. At each optical excitation wavelength, only a single antenna was strongly excited.[26] This effect is helpful to overcome the obstacle in the process of particle's transport. Because the antenna with different size corresponds to different excitation wavelength, the stable transport is impossible if the interference exists. After parameter sweep process, we choose the resonant wavelength as follows: 1190 nm, 1324 nm, 1462 nm and 1592 nm. Due to the optimal optical response and the maximum optical force is obtained at these wavelength.

3. Methods

To get accurate optical force exerted on the small particles, Maxwell stress tensor (MST) formalism is applied here.[28] The total time-averaged electromagnetic force is given by:
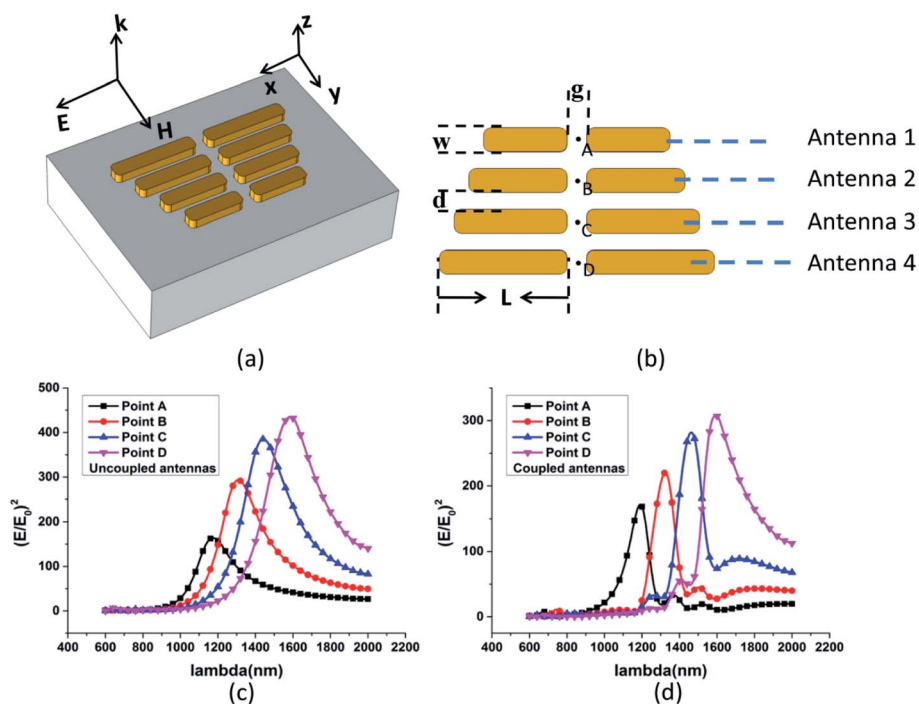

Fig. 1 (a) Schematic illustration of the Au antenna array. (b) Upper surface of the Au antenna array. (c) Field enhancement factor in central region of antennas when antennas are calculated respectively. (d) Field enhancement factor in central region of antennas when coupling effect between antennas is considered.

$$F = \oint_S \langle T \rangle \mathrm{d}S \qquad (1)$$

It is a closed surface integral in which the particle is enclosed. Maxwell stress tensor T is given by:[30]

$$\overleftrightarrow{T} = \left[\varepsilon_0 EE - \mu_0 HH - \frac{1}{2}\left(\varepsilon_0 E^2 + \mu_0 H^2\right)\overleftrightarrow{I} \right] \qquad (2)$$

where $\overleftrightarrow{I}$ denotes the unit tensor. It is worth noting that optical force derived from Maxwell stress tensor method represent the net force exerted on the particles, and ε_0 and μ_0 are the permittivity and the permeability of the medium, respectively.

The trapping potential determines the stability of the optical trap. It could derive from the optical forces. The trapping potential of a particle located at r_0 is given by:[29]

$$U(r_0) = \int_{\infty}^{r_0} F(r)\mathrm{d}r \qquad (3)$$

As we all know, Brownian motion exists in solution and it is the main interfering factor of stable trapping because the random thermal motion could release the particle out of the trap well. In theory, $1K_{B}T$ potential trap well is enough to

overcome the effect of Brownian motion[30] (K_{B} is Boltzmann's constant, and T is the temperature, we assume it 300 K here).

4. Particle transport

In this section, we analyzed the whole process of particle transport. As mentioned above, the metal antenna nanostructure could be used to trap nanoparticles because of gradient optical field. The antenna array also could be seen as several independent antennas. A whole transport process could be split into several steps as follows: as shown in Fig. 2(a), firstly, the particle is trapped by the shortest antenna at the excitation wavelength of 1190 nm. Then, the second antenna turned to resonant but the first antenna become disresonance when the excitation wavelength is switched to 1324 nm. So, the capture center moves from point A to point B. In the mean time, the force exerted on the particle drag it from point A to point B. This process could be described as the particle 'slide' into the trap well produced by the second antenna. Thirdly, the excitation wavelength is changed to 1462 nm and then the capture center is moving to point C when the particle is trapped stably at the point B. Finally, a steady transfer from point C to point D can be realized by switching the incident wavelength to 1592 nm. Fig. 2(b) shows the trapping potential diagram of transport process. Blue circles in the figures indicate the
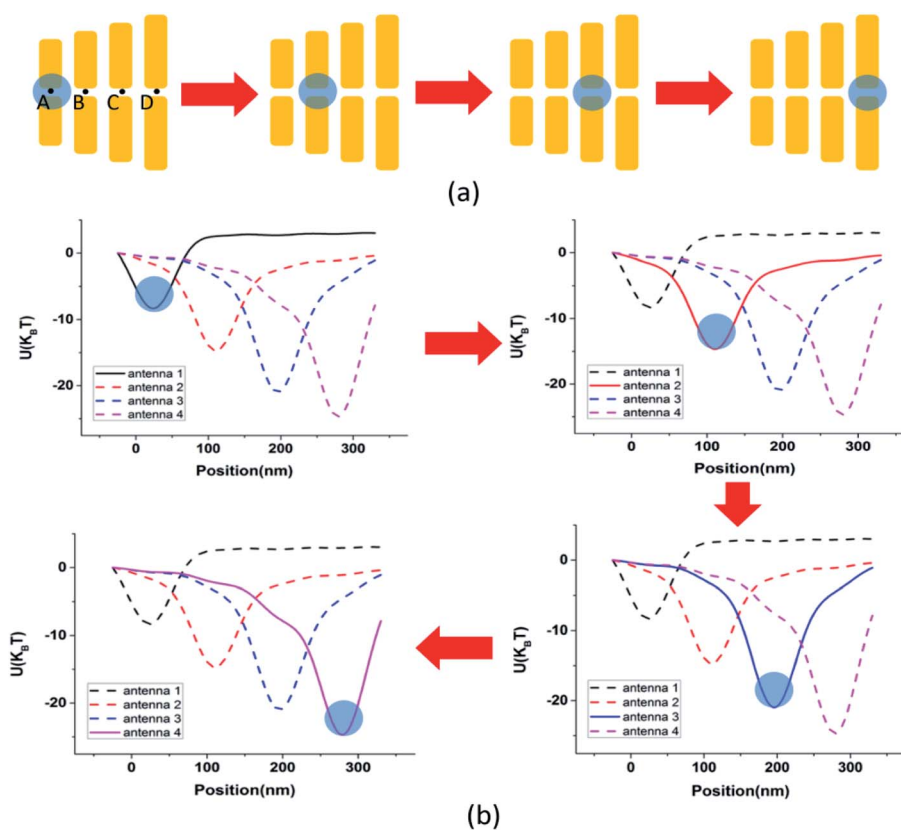

Fig. 2 (a) The transport process of nano-particles. Blue circles in the figure indicate the trapped particles in the central region of antennas. (b) The trapping potential diagram of transport process. Position of trapping potential is also changed with the wavelength of incident light. In the ideal situation, particles would be trapped in the deepest position of potential well.
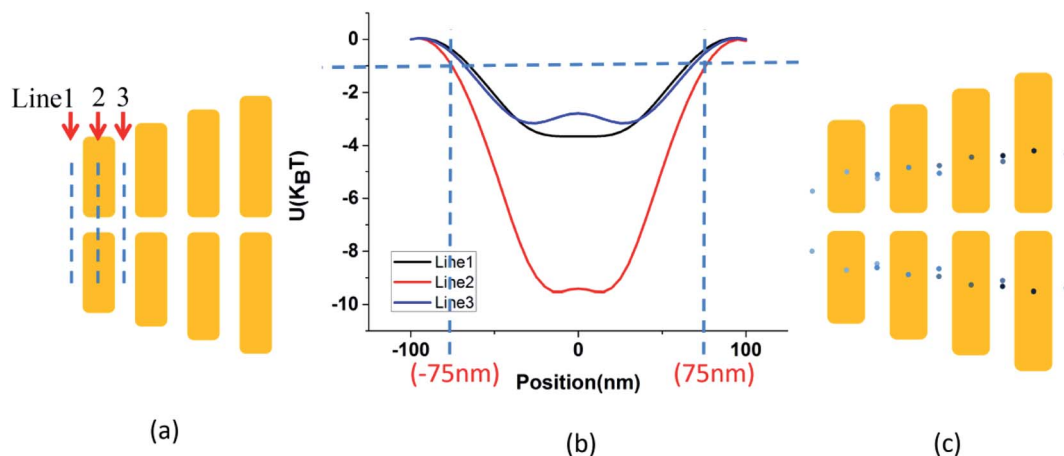
Fig. 3   (a) Dash lines in the figure are selected as calculation paths. We choose such three calculation paths for every antenna. (b) Trapping potential diagram of the lines in (a). The dash line parallel to the X axis is drawn to indicate the $1K_BT$ trapping potential and two dash lines parallel to the Y axis show the x-coordinates corresponding to the critical trapping potential depth. (c) The blue circles demonstrate the valid area we care about. The boundary points in figure are corresponding to $1K_BT$ trapping potential.

location of particles. In theory, point A, B, C and D are all capture centers so that the particles will be trapped in these points (the lowest position of the potential curve in Fig. 2(b)). The incident power intensity we used here is a modest value 5 mW μm^{-2}. The refractive index of the particle (n) was set to 2 (ref. 17) – an intermediate value between the typical refractive index of biological species such as proteins ($n = 1.6$)[31] and the II–VI quantum dots such as CdSe quantum dots ($n = 2.4$).[32] It could be used to model not only a large and low refractive index particle, but also small and high refractive index particle. The proposed structures may enable the application of biochemical diagnose and high-accuracy optical manipulation. The particle size is set as 90 nm to matching the parameter of plasmonic Au antenna array, and it is placed about 5 nm away on the upper surface of antenna array. As the particle is under a downward force at any resonant wavelength in such a distance, the whole particles we simulated in the Z plane can be regard as capturable.

5.   Valid area prediction

The all above calculations are under the condition that the particle locates in the central axis of the metal structure. However, the reality is complex, the particle may appear randomly in the solution. So it would be gratifying if we can give a certain area in which the particle could be trapped and transferred stably.

The force situation of the particle can be calculated by sweeping the position of the particle. The trapping potential is also calculated on the basis of force situation. As is shown in Fig. 3(a), take the antenna 1 as an example, the distance from particle center to central axis was changed and the particle position was swept along the dash line in the figure. The boundary line (potential is $1K_BT$ on the boundary line) was determined by calculating the trapping potential.

Fig. 3 shows the results in detailed. As is shown in Fig. 3(a), take the antenna 1 as an example, we choose three lines with different positions as the calculation paths. We calculate the force field and trapping potential applied on the particles along the three dash lines in Fig. 3(a). Results are shown in Fig. 3(b). A dash line parallel to the X axis is drawn to indicate the $1K_BT$ trapping potential and two dash lines parallel to the Y axis show the x-coordinates corresponding to the critical trapping potential depth. The two points $x = -75$ nm and $x = 75$ nm on the X axis are the critical points. It means the particles in this range would be trapped stably in the central region of antenna 1. The effective trapping range of line 1 and line 3 are calculated in the same way.

After the 12 calculation paths of the antennas were calculated, as is shown in Fig. 3(c), we can get the valid area in which the particle would be trapped and transferred stably. These boundary points, corresponding to $1K_BT$ trapping potential, were located on the structure diagram. The blue areas in the Fig. 3(c) are the valid area we desired. The particle would be trapped stably as soon as it enters to the valid area we demonstrated, it will benefits a lot in the field of biochemical diagnose and high-accuracy optical manipulation. For example, it can be used to avoid the waste of the cell or protein in the experiment and improved the efficiency greatly.

6.   Conclusion

In conclusion, we have realized a stable nanoparticles transport numerically based on a plasmonic Au antenna array. The antenna array consists of four antennas with a varying length surrounded by the water. The finite-element method is used to simulate electromagnetic field distribution, and the maxwell stress tensor is employed to calculate the optical force applied on the particles in the electromagnetic field. In addition, the trapping potential is analyzed to verify the stability of the trapped particles. We also give the valid area in which the

particles could be trapped and transferred stably by drawing the outline of boundary points with $1K_BT$ trapping potential. Our work not only provides a solution to realize the nanoparticles transport, but also predicted a valid area where the particles can be trapped. It is helpful in the field of biochemical diagnose and high-accuracy optical manipulation.

Conflicts of interest

There are no conflicts to declare.

Acknowledgements

References

1 A. Ashkin, J. M. Dziedzic, J. E. Bjorkholm and S. Chu, *Opt. Lett.*, 1986, **11**, 288–290.

2 F. m. Fazal and S. m. Block, *Nat. Photonics*, 2011, **5**, 318–321.

3 R. Bola, D. Treptow, A. Marzoa, M. Montes-Usategui and E. Martín-Badosa, *Opt. Lett.*, 2020, **45**, 2938–2941.

4 R. A. B. Suarez, L. A. Ambrosio, A. A. R. Neves, M. Zamboni-Rached and M. R. R. Gesualdi, *Opt. Lett.*, 2020, **45**, 2514–2517.

5 L.-M. Zhou, Y.-Q. Qin, Y.-J. Yang and Y.-Q. Jiang, *Opt. Lett.*, 2020, **45**, 6266–6269.

6 Y. Liu, D. K. Cheng, G. S. Sonek, M. W. Berns, C. F. Chapman and B. J. Tromberg, *Biophys. J.*, 1995, **68**, 2137–2144.

7 R. Agarwal and K. E. Duderstadt, *Nat. Commun.*, 2020, **11**, 4714.

8 H. Lina, S. J. Maerkl and O. J. F. Martin, *Opt. Express*, 2009, **17**(11), 6018–6024.

9 W.-H. Zhang, L.-N. Huang, C. Santschi and O. J. F. Martin, *Nano Lett.*, 2010, **10**, 1006–1011.

10 K. Wang, E. schonbrun, P. steinvurzel and K. B. Crozier, *Nat. Commun.*, 2011, **2**, 1480.

11 Z.-W. Kang, H.-X. Zhang, H.-F. Lu, J.-B. Xu, H.-C. Ong, P. Shum and Ho-P. Ho, *Opt. Lett.*, 2012, **37**, 1748–1750.

12 H.-R. Ding, P. S. Kollipara1, L. Lin and Y. Zheng, *Nano Res.*, 2021, **14**, 295–303.

13 O. Emile and J. Emile, *Eur. Phys. J. E*, 2020, **43**, 11991.

14 A. N. Grigorenko, N. W. Roberts, M. R. Dickinson and Y. Zhang, *Nat. Photonics*, 2008, **2**, 365–370.

15 M. L. Juan1, M. Righini1 and R. Quidant, *Nat. Photonics*, 2011, **5**, 349–356.

16 Y.-Z. Shi, H.-T. Zhao, L. K. Chin, Yi Zhang, P. H. Yap, W. Ser, C.-W. Qiu and A.-Q. Liu, *Nano Lett.*, 2020, **20**, 5193–5200.

17 A. A. E. Saleh and J. A. Dionne, *Nano Lett.*, 2012, **12**, 5581–5586.

18 M. Ploschner, M. Mazilu, T. F. Kraussc and K. Dholakiad, *J. Nanophotonics*, 2010, **4**, 041570.

19 X.-D. Yang, Y.-M. Liu, R. F. Oulton, X.-B. Yin and X. Zhang, *Nano Lett.*, 2011, **11**, 321–328.

20 T. Chantakit, C. Schlickriede, T. Weiss, N. Chattham and T. Zentgraf, *Photonics Res.*, 2020, **8**, 1435–1440.

21 Y. Li, G.-H. Rui, S.-C. Zhou, B. Gu, Y.-Z. Yu, Y. P. Cui and Q.-W. Zhan, *Opt. Express*, 2020, **28**, 27808–27822.

22 B. Melo, F. Almeida, G. Temporao and T. Guerreiro, *Opt. Express*, 2020, **28**, 16256–16269.

23 P. Hansen, Y. Zheng, J. Ryan and L. Hesselink, *Nano Lett.*, 2014, **14**, 2965–2970.

24 Y. Zheng, J. Ryan, P. Hansen, Y.-T. Cheng, T.-J. Lu and L. Hesselink, *Nano Lett.*, 2014, **14**, 2971–2976.

25 Z.-w. Kang, H.-F. Lu, J.-J. Chen, K. Chen, F. Xu and Ho-P. Ho, *Opt. Express*, 2014, **22**, 19567–19572.

26 S. Zhang, Z.-L. Ye, Y. Wang, Y. Park, B. Guy, M. Mrejen, X.-B. Yin and X. Zhang, *Phys. Rev. Lett.*, 2012, **109**, 259902.

27 E. D. Palik, *Handbook of optical constants of solids*, Academic Press, 1998, vol. 3.

28 L. Novotny and B. Hecht, *Principles of nano-optics*, 2012, Cambridge University Press.

29 L. Novotny, R. X. Bian and X. Sunney Xie, *Phys. Rev. Lett.*, 1997, **79**, 645–648.

30 A. H. J. Yang, T. Lerdsuchatawanich and D. Erickson, *Nano Lett.*, 2009, **9**, 1182–1188.

31 T.-L. McMeekin, M.-L. Groves and N.-J. Hipp, Amino Acids and Serum Proteins, in *Advances in Chemistry*, American Chemical Society, Washington, DC, 1964, vol. 44, ch. 4, pp. 54–66.

32 L.-W. Wang and A. Zunger, *Phys. Rev. B: Condens. Matter Mater. Phys.*, 1996, **53**, 9579–9582.